Surface & Coatings Technology 258 (2014) 832–841

Contents lists available at ScienceDirect

Surface & Coatings Technology

journal homepage: www.elsevier.com/locate/surfcoat

Development of ultra-strong adhesive strength coatings using cold spray

Renzhong Huang *, Wenhua Ma, Hirotaka Fukanuma

Plasma Giken Co., Ltd., Toshima, Tokyo, Japan

ARTICLE INFO

Article history:
Received 25 March 2014
Accepted in revised form 24 July 2014
Available online 4 August 2014

Keywords:
Cold spray
Adhesive strength
Copper coating
Splat
Fracture surface

ABSTRACT

In the cold spray process, adhesive strength between coatings and substrates is considered to be the most crucial mechanical property. Bonding is an important factor in determining if cold spray can be used for an application. Therefore, development of effective bonding between coatings with various substrates is essential to cold spray processing. In this study, Cu coatings were deposited on to three different substrates: Al5052, Al6063, and stainless steel 316 L. The adhesive strength of Cu coatings on these three substrates was investigated. The experimental results showed that effective bonding could be generated only when particle velocity exceeds 500 m/s for Al alloy substrates, and 800 m/s for stainless steel 316 L substrates. Based on the present studies, an ultra-strong bonding (more than 200 MPa) between dissimilar materials has been developed with cold spray processing.

1. Introduction

Cold spray is an emerging spray coating technology that was first developed in the mid-1980s at the Institute of Theoretical and Applied Mechanics in the former Soviet Union [1]. Cold sprayed coatings can be achieved only when the velocity of in-flight particles exceed a certain critical velocity [2,3]. Therefore, the velocity prior to impacting the substrate is the most important parameter in cold spray [4]. Compared to traditional thermal spray processes, particles go through intensive plastic deformation upon impact in solid states at temperatures well below their melting point. Therefore, cold spray is particularly suitable to prepare coatings that are sensitive to oxidation [5].

Adhesive strength of coatings prepared by cold spray determines its applications in the industrial field. Many researches have been performed to focus on the bonding mechanism of cold spray, but it still remains unclear [6–19]. Mäkinen et al. presented the influences of powder, substrate and heat treatment on adhesive strength [6]. Donner et al. examined the effects of chemical affinities and hardness of substrate on adhesive strength [7]. Moreover, recent numerical simulation also has helped to explore the bonding mechanism [8–15]. These studies on bonding mechanism of cold spray suggested that adhesive strength is mainly affected by mechanical interlock [7–9,16] and metallurgical bonding caused by impact molten or diffusion bonding [11–19] based on the shear instability [10]. One of the purposes to study the bonding mechanism is to prevent coating de-bonding from substrate. De-bonding of coating in thermal spray is mainly caused by its residual stress, and the increased thickness aggravates the de-bonding tendency owing to the accumulation of residual stress [20,21]. For cold spray, Fukanuma and Ohno also experimentally demonstrated that by increasing coating thickness, it increases the risk of separation between coating and substrate due to the accumulated internal stress [22]. Effective bonding can be formed between coating and substrate only in the case where there is adequate adhesive strength to overcome the internal stress [21–23].

Adhesive strength measurements for cold spray coatings are carried on by pull tests, e.g. according to the standard: EN582 Thermal Spraying. In the conventional test, an epoxy resin adhesive is employed to glue specimen with a loading block. The reliability of the test depends on this glue's strength. Due to the restriction of test method and cold spray equipment's capability, the adhesive strength of cold-sprayed coatings reported has no more than 70 MPa. Even though Smurov et al. put forward a new method by pulling a specially machined specimen to break through the restriction of the conventional adhesive strength test, the adhesive strength was still less than 30 MPa due to the non-optimized spray conditions [24]. Studies about ultra-strong adhesive strength of cold-sprayed coating have not been reported up to now.

In our previous study, an adhesive strength test method similar to the one of Smurov was put forward [25,26]. In the present study, the adhesive strength of Cu coatings on Al5052, Al6063 and stainless steel 316 L substrate was measured. Particle velocities were calculated by one-dimensional isentropic model. Moreover, relationships between the particle velocity and the adhesive strength of Cu coatings were

* Corresponding author.
E-mail address: rz_huang@plasma.co.jp (R. Huang).

http://dx.doi.org/10.1016/j.surfcoat.2014.07.074
0257-8972/

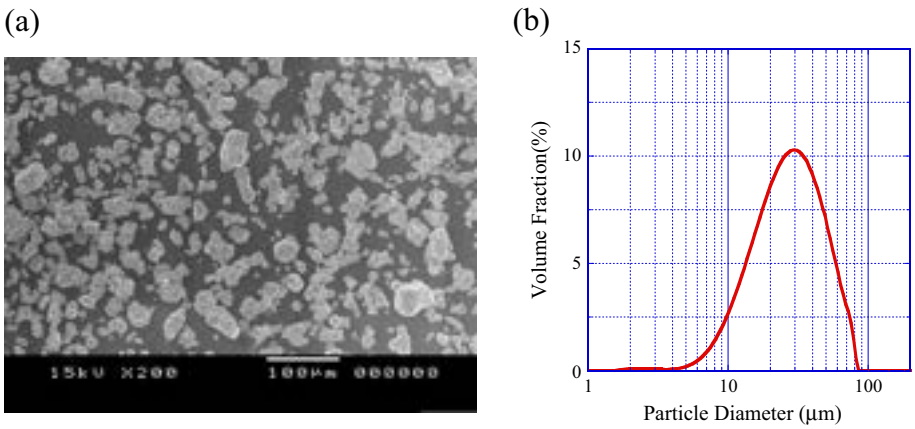

Fig. 1. Morphology (a) and diameter distributions (b) of Cu powder for adhesive strength coatings.

discussed. In order to understand the bonding mechanism of cold spray process, splats were also observed. A way to develop the ultra-strong adhesive strength of cold-sprayed coating was established.

2. Experimental procedures

2.1. Feedstock powder and cold spray process

Commercially available water atomized Cu powder (Cu-Atw-350 mesh, Fukuda Metal Foil & Powder Co., Ltd.) was used to prepare the coatings for adhesive strength test. The morphology of the powder is presented in Fig. 1(a) and the volume distributions of particle diameter are shown in Fig. 1(b). Powder is near spherical shaped and its diameter ranges from 5 to 80 μm with a volumetric average diameter of 28 μm.

In order to restrict the deviation of splat, customized high-pressure water atomized Cu powder (Mitsui Mining & Smelting Co., Ltd.) was used as the feedstock to deposit the splat. The morphology of the powder is shown in Fig. 2(a). Volumetric distributions of particle diameter are shown in Fig. 2(b). The powder presents a perfectly spherical shape and the diameter ranges from 20 to 50 μm with a volumetric average diameter of 33 μm.

Cold spray system PCS-1000 was used to prepare the splat for observation and coatings for adhesive strength test. A convergent–divergent (De-Laval) nozzle was configured in the cold spray system to accelerate the working gas to supersonic speed. This nozzle is cooled by water in order to alleviate nozzle clogging which highly improves the reliability of this system. In the current cold spray system, the preheated working gas (high temperature) is mixed with the powder feeding gas (room temperature) before flowing into the convergent section of the nozzle. The mixed gas temperature is regard as the inlet gas temperature flowed into the nozzle that determines the gas speed at the nozzle throat. In order to control the mixed gas temperature (or the gas velocity at the nozzle throat), powder feeding gas to working gas flow rate ratio was set to about 1/4–1/5. Both helium and nitrogen gas were employed as working gas. The working gas pressures were controlled ranging from 2 to 5 MPa and the working gas temperatures ranging from 473 to 1273 K to achieve different particle velocities. A planar robot program was used to spray adhesive test coatings with transverse speed of 300 mm/s and step of 1 mm. Splats were sprayed by a line movement robot program with the speed of 800 mm/s. Substrates were placed about 30 mm away from the gun exit for both spraying processes of the coatings and the splats.

Al5052, Al6063 and stainless steel 316 L were utilized as substrates. According to the previous studies, sandblasting did not benefit the bonding of cold-sprayed coating [16,27]. The coatings for adhesive strength test were deposited on machined substrates without sandblasting. Tensile strength of substrates was measured with the tensile testing equipment AG-X (100KN), manufactured by Shimadzu Co., Ltd. Dimensions of the substrate tensile specimens are shown in Fig. 3(a) following the standards of No. 14B according to JIS Z2201 and the measured mechanical properties are shown in Fig. 3(b). It can be seen that the tensile strength of stainless steel 316 L substrate exceeds 600 MPa,

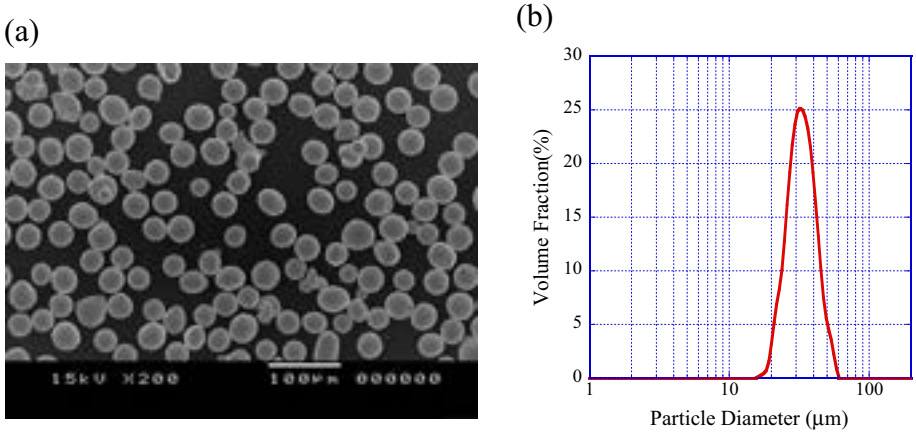

Fig. 2. Morphology (a) and diameter distributions (b) of Cu powder for preparing splat.

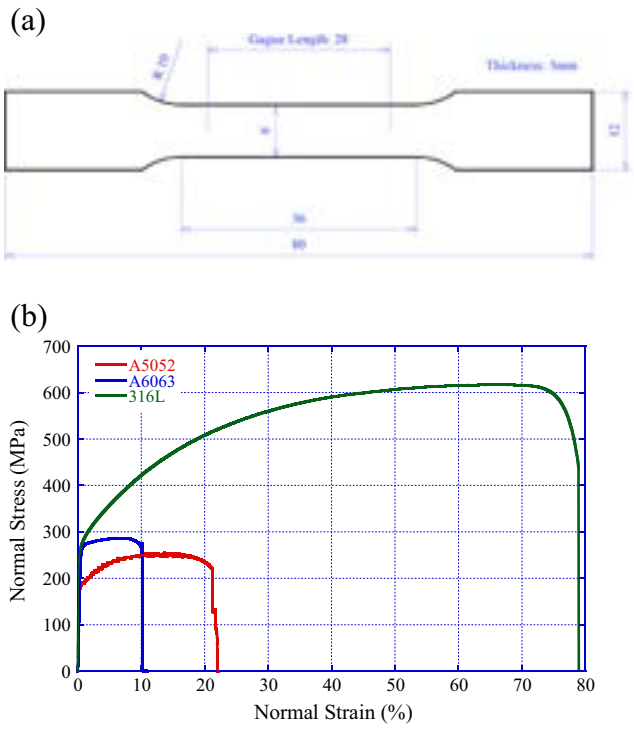

Fig. 3. Dimension of tensile specimen (a) and tensile strength (b) of substrate.

which is more than twice of the other two Al alloys. The tensile strength of Al6063 is a little stronger than the Al5052 substrate.

2.2. Particle velocity

In our previous study, the steady-state one-dimensional isentropic model can predict the particle velocity for the water-cooling cold spray system with an acceptable accuracy [25]. Therefore, in this study, the steady-state one-dimensional isentropic model was used to calculate the gas flow inside the De-Laval nozzle in order to simplify the calculation. Gas is considered as perfect and compressible gas, and the nozzle is regarded as adiabatic wall so that no heat loss occurs to the surroundings. The dimension of nozzle calculated in this study is similar to the one given in Ref. [26]. Based on the above assumptions, Mach number, gas velocity and temperature can be obtained with nozzle dimension [28]. Once the gas temperature and velocity are characterized, the particle acceleration and heat transfer to the particles can be calculated. In the present study, particle velocity at the nozzle exit was considered as a typical particle velocity instead of its impacting velocity onto the substrate in order to simplify the calculation. The detailed method to calculate the particle velocity and temperature are given in Refs. [29] and [30].

2.3. Splat characterization

In this study, the cross sections of splatted Cu particles were prepared perpendicularly to their surfaces by a commercially available apparatus called Cross Section Polisher (SM-09020CP, JEOL, Japan) using a broad ion beam. The method minimizes the artifacts such as exaggerated densification and/or reduced porosity, which can be induced by the smearing of sprayed metallic powder particles during sample preparation [31]. The acceleration voltage and milling speed of the Cross Section Polisher were 4 kV and 50 μm/h respectively, under the chamber pressure of 2×10^{-3} Pa. Morphologies and prepared cross sections of the splatted copper particles were examined by an emission scanning electron microscope (JSM-5200LV, JEOL, Japan).

2.4. Adhesive strength test

In the conventional adhesive strength test for thermal spray coatings, an epoxy resin adhesive is employed to glue the sample to a loading block. The test results are tremendously restricted by the strength of glue. The adhesive strength of epoxy resin is generally not higher than 70 MPa. Consequently, the testing method cannot be employed to measure coating adhesions with a higher adhesive strength than that of the adhesive.

For cold spray process, a suitable spray condition can prepare coatings with high adhesive strength [26]. Therefore, the conventional testing method became invalid for the high adhesive strength coatings prepared by cold spray process. Fortunately, it is possible to build thick coatings by cold spray process. The cold-sprayed coating can be machined and pulled to measure the adhesive strength [24–26]. In this study, the same tensile test method to our previous studies was adopted. The detailed dimensions and test procedures were given in Refs. [25] and [26].

3. Results

3.1. Particle velocity

With the powder average diameter of 28 μm, the calculated particle velocities (at the nozzle exit) under different working gas temperatures and pressures are shown in Fig. 4. It can be seen that particle velocity ranged from about 500 to 700 m/s with nitrogen gas and from about

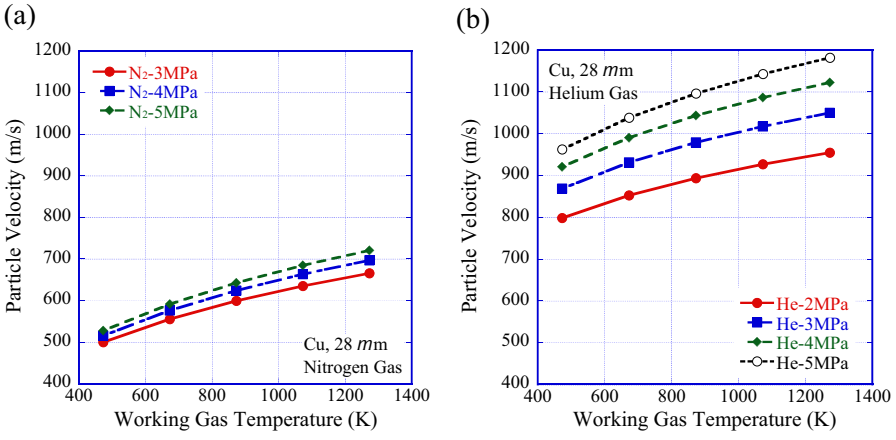

Fig. 4. Particle velocity accelerated by N2 (a) and He (b).

800 to 1200 m/s with helium gas. Particle velocity increased as both gas temperature and pressure increased. Higher gas temperature leads to higher sonic speed at the nozzle throat (consequently higher gas velocity inside the nozzle). Higher gas pressure leads to higher gas density inside the nozzle (consequently a larger gas drag force to the particle). Both increases in gas velocity and density benefit to improving particle velocity. Since the sonic speed of helium gas is much higher than that of the nitrogen gas, particle velocities accelerated by helium gas are far higher than those of nitrogen.

3.2. Splat

Fig. 5 shows the morphologies and cross-sections of the cold-sprayed Cu splats on Al5052 substrate under different working gas temperature, keeping the gas pressure at 3 MPa. It can be seen that particle re-bounded from the substrate and only some craters remained in the substrate when the gas temperature is less than 473 K. It seems that it is difficult to deposit to Al5052 substrate at N2, 3 MPa, 473 K condition, since the particle velocity is low. With the increase of working gas

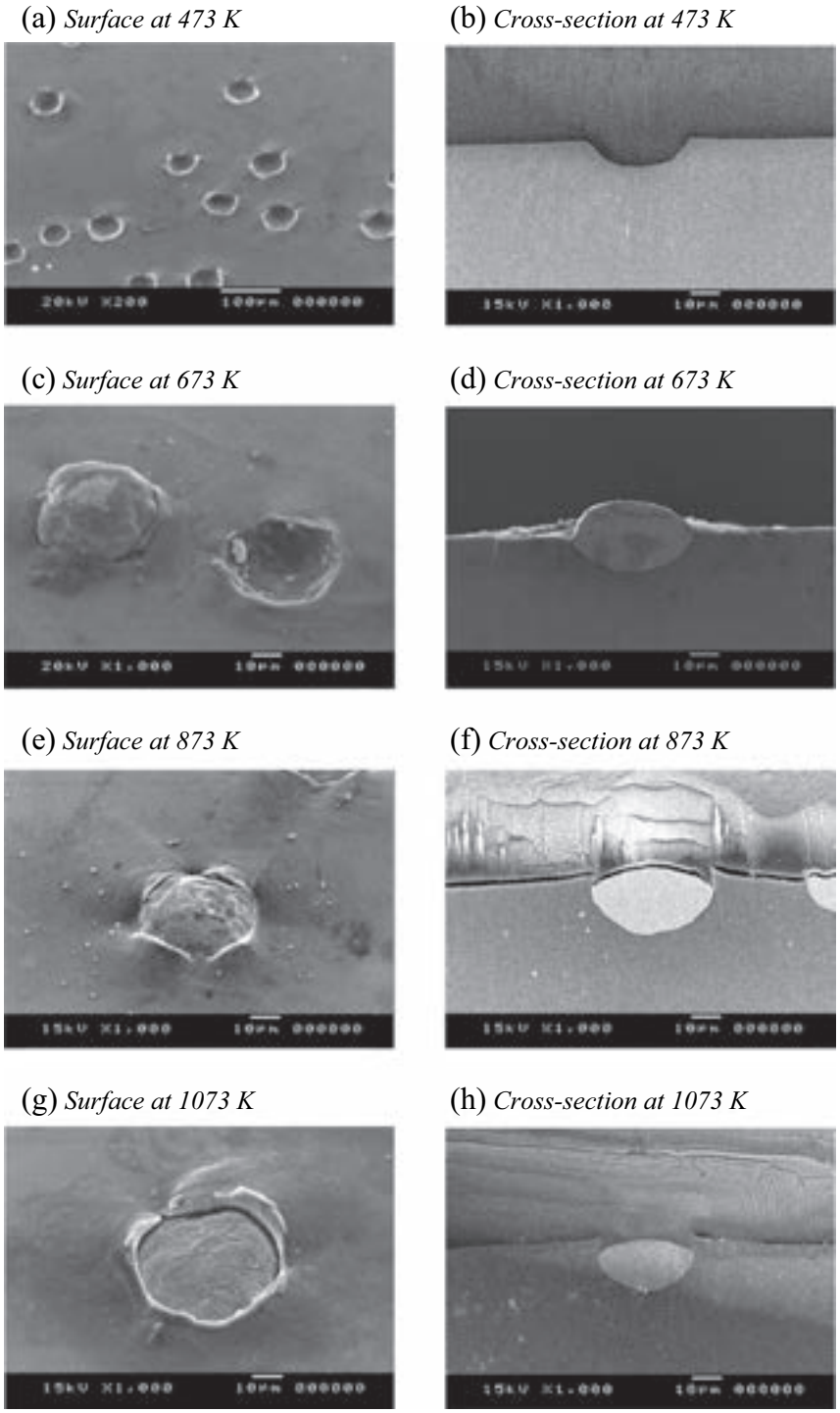

Fig. 5. Morphologies (a, c, e, and g) and cross-sections (b, d, f, and h) of Cu splats sprayed on Al5052 substrate at working gas pressure of 3 MPa and different gas temperatures.

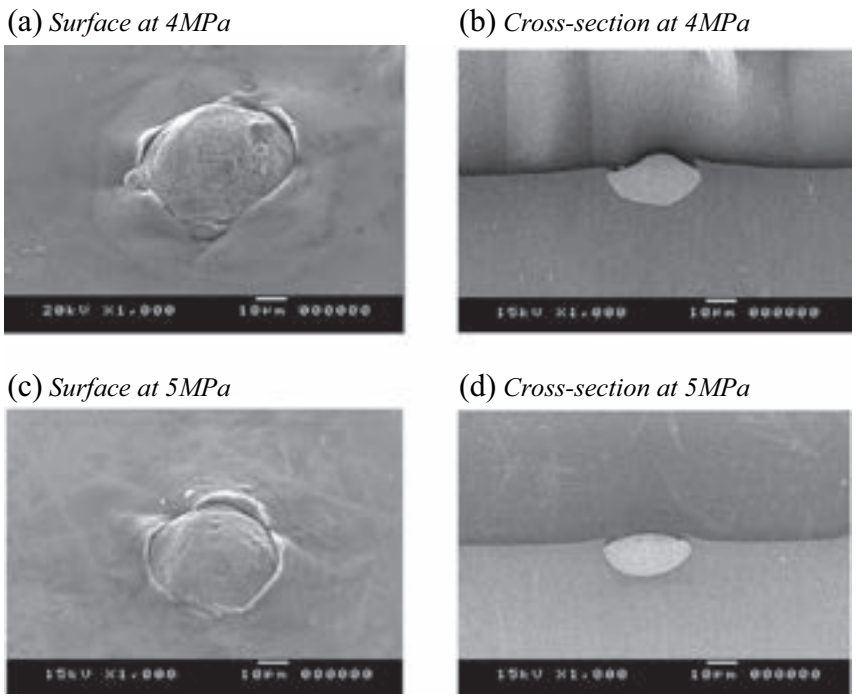

Fig. 6. Morphologies (a and c) and cross-sections (b and d) of Cu splats sprayed on Al5052 substrate at working gas temperature of 673 K and different gas pressures.

temperature, not only the Cu particles were deposited on to the substrate, but also they were embedded into the substrate owing to the increased particle velocity. Jetting can be observed when the gas temperature exceeds 873 K as shown in Fig. 5(f) and (h).

Fig. 6 shows the morphologies and cross-sections of the Cu splats on the substrate of Al5052 under different working gas pressure keeping the gas temperature of 673 K. Together with Fig. 5(c) and (d), it can be seen that the particles are embedded into the substrates more deeply when the working gas pressure is increased from 3 to 5 MPa. This is caused by increase in particle velocity and the softening of substrate (more sufficient heat exchange between gas and substrate) at a higher gas pressure. A small jetting can be observed for the Cu splat at the gas pressure of 4 MPa as shown in Fig. 6(b), and the jetting became more remarkable when the working gas pressure was increased to 5 MPa as shown in Fig. 6(d).

Fig. 7 shows the morphologies and cross-sections of Cu splats on Al6063 substrate at working gas pressure of 3 MPa and gas temperature of 873 K with nitrogen gas. Compared with the Cu splat on Al5052 substrate as shown in Fig. 5(e) and (f), it seems that no significant difference can be observed between the two Al alloy substrate of Al5052 and Al6063. Fig. 8 shows the morphologies and cross-sections of Cu splats on stainless steel substrate at working gas pressure of 3 MPa and gas temperature of 673 K with nitrogen gas. It can be seen that Cu particle underwent severe deformation and almost no deformation with the stainless steel substrate. According to the studies of Bae, plastic energy is primarily dissipated onto the softer counterpart when a hard material impacts with a soft material [32]. As a result, the deformation mostly happens to the softer Cu particle instead of the harder stainless steel substrate.

Fig. 9 shows the morphologies and cross-sections of Cu splats on Al5052 and stainless steel substrates with working gas pressure of 3 MPa and temperature of 673 K with helium gas. Compared with the Cu splats as shown in Figs. 5(c) and (d) and 8, it can be seen that splats on the two substrates are much more embedded when helium is being used. The particle velocity with helium is much higher than that of the nitrogen gas. As a result, splats were embedded deeper. Even though the substrate of stainless steel is significantly harder, the Cu particle caused some deformation of the substrate with its higher particle velocity as shown in Fig. 9(c) and (d), consequently embedded into the substrate to some degree.

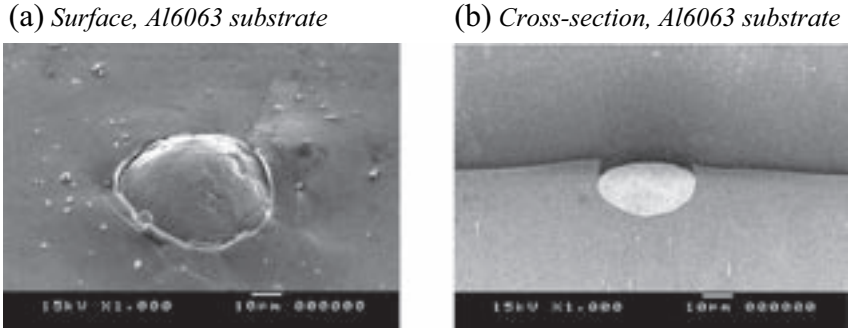

Fig. 7. Morphologies (a) and cross-sections (b) of Cu splats sprayed Al6063 substrate at working gas temperature of 873 K and pressure of 3 MPa with nitrogen gas.

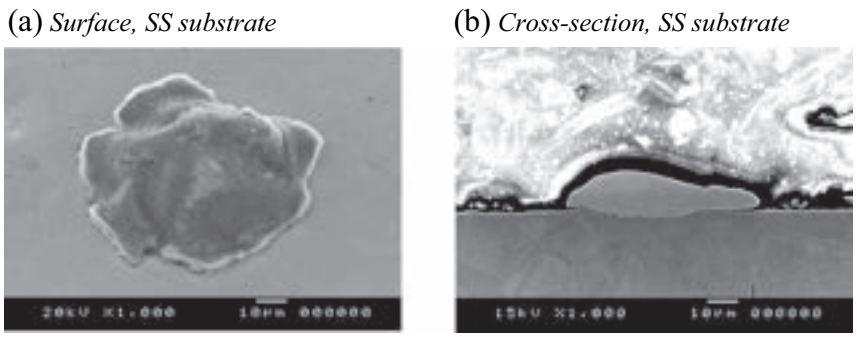

Fig. 8. Morphologies (a) and cross-sections (b) of Cu splats sprayed on SS substrate at working gas temperature of 673 K and pressure of 3 MPa with nitrogen gas.

3.3. Adhesive strength

Adhesive strength of Cu coatings on the three substrates is shown in Fig. 10. It can be seen that the tensile strength increased with its gas temperature. The gas pressure hardly has any effect on the adhesive strength for Al5052 and Al6063 substrates when nitrogen gas is used (especially under lower working gas temperature as shown in Fig. 10(a) and (b)). On the other hand, when helium gas was employed as the working gas, the tensile strength of coatings on Al alloy substrates was much higher. For stainless steel substrates, the coatings deposited by nitrogen gas were separated from the substrates, and the measured adhesive strength of helium gas is shown in Fig. 10(c). It is obvious that the tensile strength increased significantly with the helium gas pressure owing to the increased particle velocity. High particle velocity can generate an ultra-strong adhesive strength of Cu coatings (more than 200 MPa) even on stainless steel substrates.

Although the current test method can measure the coatings with high adhesive strength, another problem in the test process became clear. When adhesive strength between the coatings and substrates is extremely strong, during the tensile test, rupture will then occur inside the coatings instead of the interface as shown in Fig. 11. One of the reasons to cause failure within the coatings is stress concentration. In spite of the arc transition used at the inner corner near the interface of coating/substrate, the stress concentration may have caused some failures of specimens near the inner corner. Another reason is the inherent defects in the cold-sprayed coatings. These defects are so sensitive to the tensile stress that the cohesive strength of coatings decreases intensively. Consequently, when the adhesive strength is stronger than the cohesive strength of coatings, rupture inside the coatings appears.

4. Discussion

It has been commonly accepted that the bonding between substrate and the cold-sprayed coating is based on the intensive plastic deformation of substrate and particle during the impacting process. The intensive localized deformation causes adiabatic shear instability at the interface, and consequently material extrudes from the interface and forms a metal jet at the rim. Upon impact, the thin oxide film at the interface is broken and clean interface is formed [2,8,10,12,14]. The

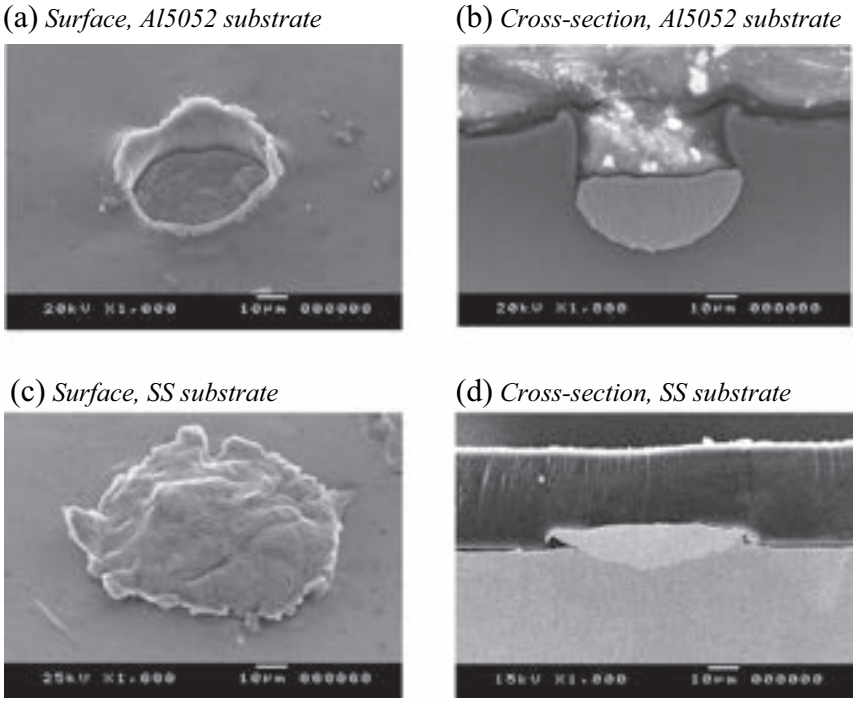

Fig. 9. Morphologies (a and c) and cross-sections (b and d) of Cu splats sprayed on Al5052, and SS substrate at the working gas temperature of 673 K and pressure of 3 MPa with helium gas.

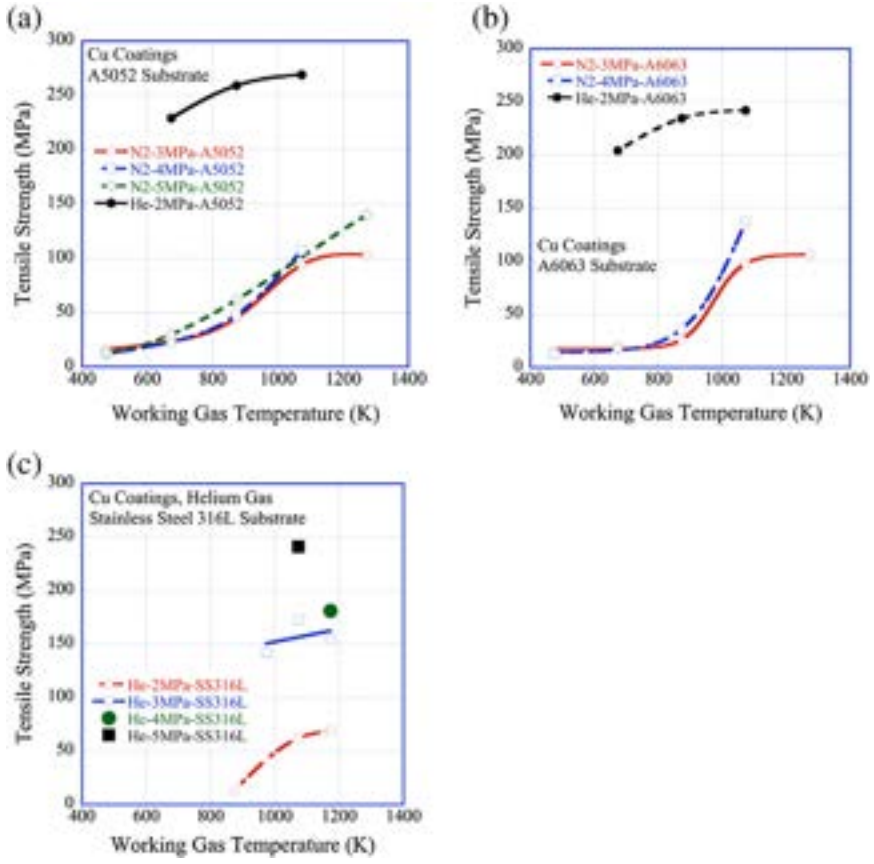

Fig. 10. Tensile strength of adhesive test on Al5052 (a), Al6063 (b) and SS 316 L (c) substrates.

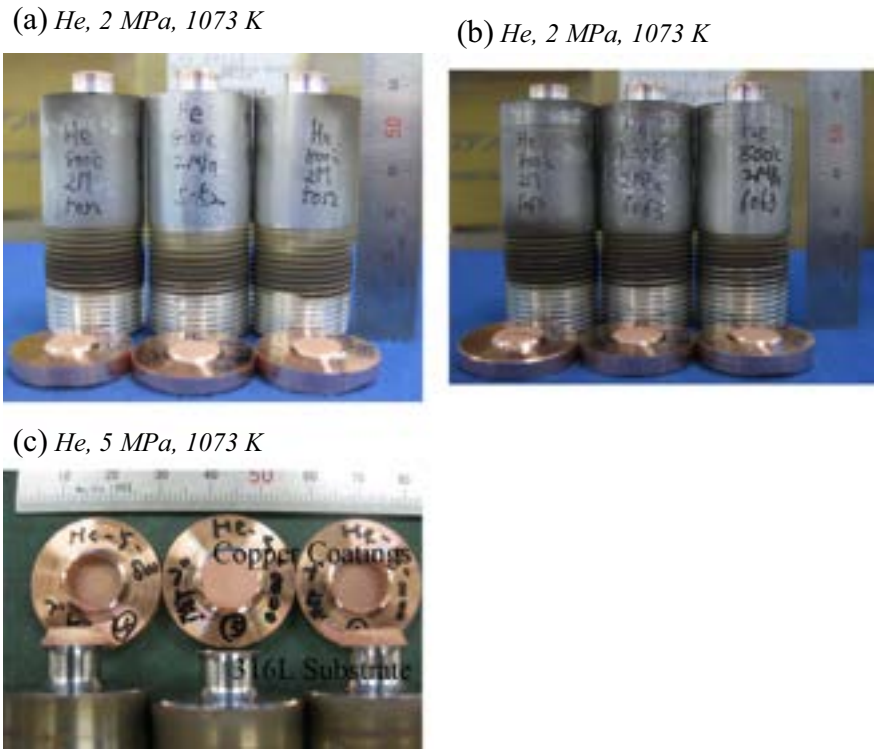

Fig. 11. Ruptured specimen photos of Al5052 (a), Al6063 (b) and SS316L (c) substrates.

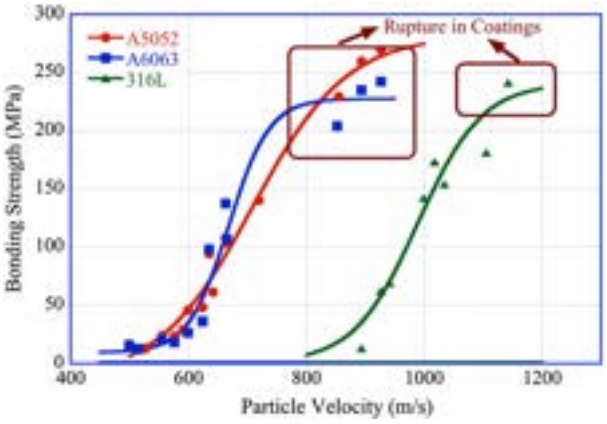

Fig. 12. Relationship between particle velocity and adhesive/tensile strength.

effective bonding attributes to mechanical interlock caused by the mixture of substrate and coating materials at the interface region [8, 26] and the true metallurgical bonding at the clean fresh interface based on local high temperature caused by the strain heating similar to the explosive welding [11,14–16]. Even though the increased particle and substrate temperature benefits to the coating process [13], particle velocity is the most important parameter to influence bonding [19]. Fig. 12 shows the relationship between the tensile strength (from Fig. 4) and the calculated particle velocity (from Fig. 10). It reveals that only when particle velocity exceeds a certain value (critical velocity), effective bonding can be obtained. It seems that the substrate materials tremendously affect effective bonding that higher particle velocity is necessary for higher strength substrate. Cu coating can effectively be bonded with Al alloy substrate if particle velocity is more than 500 m/s and stainless steel substrate with particle velocity of more than 800 m/s (as shown in Fig. 12). Fig. 4 reveals that it is difficult to acquire particle velocity more than 800 m/s with nitrogen gas using the current cold spray system. Therefore, Cu coatings deposited with nitrogen gas separated from the stainless steel substrates.

The adhesive strength increases slowly when particle velocity is a little higher than critical velocity, and then sharply increases with the particle velocity as shown in Fig. 12. When the adhesive strength reaches to the point where it is stronger than the cohesive strength of the inside coating, adhesive strength cannot be tested using the current test method due to the rupture location inside the coatings as shown in Fig. 11. Considering the rupture position and the stress concentration at the inner corner of tensile specimen, Fig. 12 only shows the lower limit of its adhesive strength of coating/substrate at the higher particle velocity region. The real adhesive strength should be stronger than the measured one. Even so, conclusion can be drawn that adhesive strength benefits from an increase in particle velocity. The results agree well with Dr. Schmidt's report that particle velocity is the most important parameter to determine the bonding in cold spray process [19].

Ultra-strong adhesive strength can be explained by observing the morphologies of Cu splat on the three substrates. For Al alloy substrate, with the increase in particle velocity, Cu particles get deeply embedded into the substrate, which causes intensive plastic deformation in both the particles and the substrates as shown from Figs. 5 to 7. With the deformation of Al substrate, an inward jetting of substrate is formed at the rim of the particle. Unlike the splat (which is only one particle impacting on to the substrate), in the cold spraying process, particle will impact on jets and mechanical interlock will happen. Fig. 13 shows the cross-sections of Cu coatings on Al alloy substrates. It can be seen that interlock was formed at Cu/Al alloy interface. Moreover, the interlock effect becomes more remarkable with the increase in particle velocity (compared at Fig. 13(a) and (b)).

During the impact process of Cu particle on Al alloy substrate, not only did the deformation and metal jetting occur, but also intermetallic compounds (Al_2Cu and Al_4Cu_9) were formed at the interface [11]. The intermetallic compounds of Al and Cu are brittle and low in strength [33]. Therefore, even though the metallurgical bonding based on diffusion was formed at the interface of Cu coating and Al substrate, the mechanical interlock is able to account for a large proportion of the total bonding strength in most cases [16]. In the present study, it is considered that interlock plays a key role in bonding instead of its metallurgical bonding. Fig. 5 shows that jetting was almost unobservable under the conditions of N_2, 3 MPa, 673 K, and jetting was obtained when the gas temperature was increased to 873 K. Fig. 6 reveals that the increased gas pressure makes the particle more deeply embedded into the substrate due to the increased particle velocity. Unlike the one when the gas pressure was increased, by increasing the gas temperature, it more effectively embedded the particle into Al5052 substrate (compared at Figs. 5 and 6). One reason is because gas temperature affects the particle velocity more with nitrogen gas (shown in Fig. 4(a)). Another reason is that by increasing the gas temperature, it softens the particle and the substrate by heat. With particles deeply embedding into the substrate, it increases the material mixing (interlock) at the interface. Consequently, this gives higher interface bonding strength [8]. Therefore, the increase of gas temperature is more effective in improving the adhesive strength than that of gas pressure if nitrogen gas is used as shown in Fig. 10(a) and (b). If particle velocity increased further with helium gas, particles are embedded more into the Al5052 substrate as shown in Fig. 9(a) and (b). The severe mechanical interlock resulting from intensive plastic deformation leads to high adhesive strength (more than 250 MPa on Al5052 substrate). For Al6063 substrate, the splat is very similar to the one from the Al5052 substrate as shown in Fig. 7.

(a) *Al6063 substrate, N_2, 3MPa, 1273 K* (b) *Al6063 substrate, He, 2MPa, 1073 K*

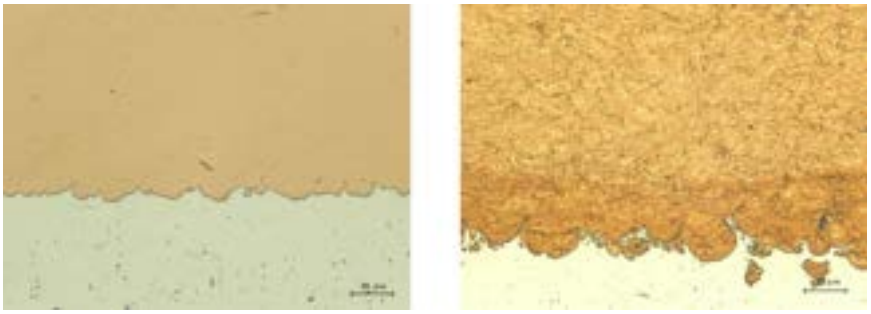

Fig. 13. Cross-sections of Cu coatings on Al alloy substrates.

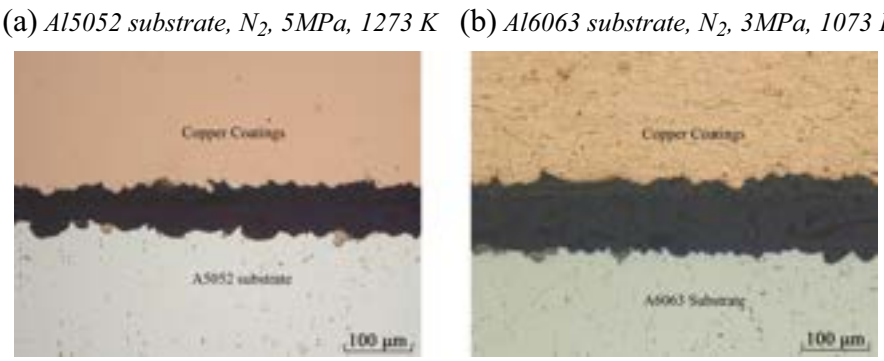

Fig. 14. Cross-sections of fractured Cu coatings on Al alloy substrates.

Therefore, the relationship between particle velocity and adhesive strength for the two Al alloy substrates looks very similar as shown in Fig. 12. Fig. 14 shows the cross-sections of fractured Cu coatings on Al alloy substrates. The Cu particles that remained on the substrates are deeply embedded and Al alloy substrate is also inlaid in the coatings between the Cu particles (shown in Fig. 14(a)). This proves that there is intensive interlock between the Cu coating and Al alloy substrate.

The adhesive strength on Al alloy substrate sharply increased when the particle velocity exceeded about 600 m/s (as shown in Fig. 12). Observing the splat on Al alloy substrate, the jetting are not remarkable if the spray temperature is less than 873 K and particle velocity less than 600 m/s (as shown in Fig. 4). Consequently, the interlock effect will not be significant between the coating and substrate and only weak bonding can be obtained. This weak bonding maybe generate from the friction between substrate and coating [34]. Even though these substrates were not prepared with sandblasting, the particle impact process made the substrate surface rough (enough to form a weak mechanical bonding based from friction). With the increase of impact velocity, the inward jetting formed on softer Al alloy substrate surface due to particle's inset. And consequently, particle is almost enclosed by the substrate. This generated a significant interlock effect at the interface of Cu coating and Al alloy substrate (as shown in Fig. 13(b)), and stronger adhesive strength can be observed.

For stainless steel substrates, the substrate is so strong that it is difficult to make the substrate deform since deformation always happens to the softer counterpart during impact [32]. Therefore, it is difficult to deposit Cu coating on stainless steel substrates. Even when helium gas was used to deposit Cu coating on stainless steel substrate, it did not deform as much as Al alloy substrate (as shown in Fig. 9). Therefore, the interlock effect for the bonding between Cu particle and stainless steel substrate seems difficult. However, a strong adhesive strength (more than 200 MPa) on stainless steel substrate can still be acquired. Effective bonding between Cu particle and the stainless steel substrate may be mainly attributed to their metallurgical bonding. The strain heat can be generated during the high velocity particle impact of Cu particle on the stainless substrate and local temperature can be close to the melting point [14,19]; like pressure welding, strong diffusion bonding or metallurgical bonding can be formed [35–37]. Fig. 15 shows the cross-sections of fractured Cu coatings on stainless steel substrates. It can be seen that some Cu particles still remained on the stainless steel substrate even though they did not deeply embed into the substrate. Observing the surface of the stainless steel 316 L substrate after the fracture in Fig. 16, it can be also seen that plenty of Cu coatings remained on the substrate. Also, the fracture occurred in the coating/substrate interface and partly inside of the Cu coatings. It seems that bonding strength is stronger than the cohesive strength of Cu coating at part of the coating/substrate interfaces and weaker at other interfaces. The impacting particle velocity being uneven causes the difference in bonding strength for different particles. The different particle velocities attribute to the particle diameter distribution and the different trajectory of particle inside the nozzle [11]. The increased gas pressure overall improves particle velocity and increases the bonding between the particles and the substrates by generating more strain heat and more adequate diffusion. Therefore, the remained particles sprayed under 3 MPa are much more than those sprayed under 2 MPa (as shown in Fig. 16). It can be also seen from Fig. 16 that few large particles remained on the substrate at 2 MPa compared with the ones at 3 MPa because small particles are easier to get a higher velocity. With the increase of gas pressure (from 2 to 3 MPa), not only the interface bonding increased, but also the cohesive strength of Cu coating improved. The increased adhesive and cohesive strength benefited to the measured tensile strength when helium gas pressure increased from 2 to 3 MPa.

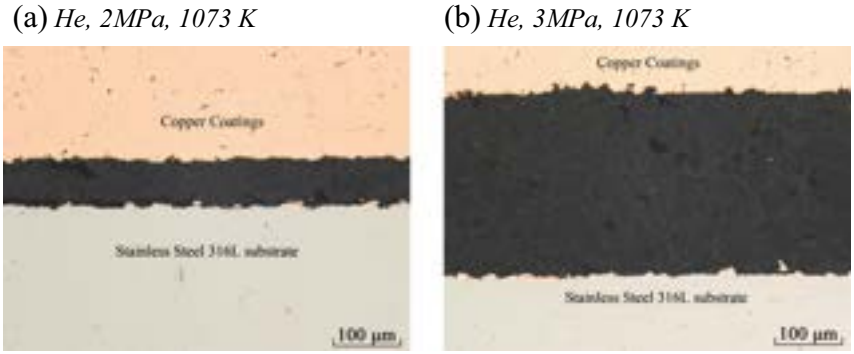

Fig. 15. Cross-sections of fractured Cu coatings on SS 316 L substrates.

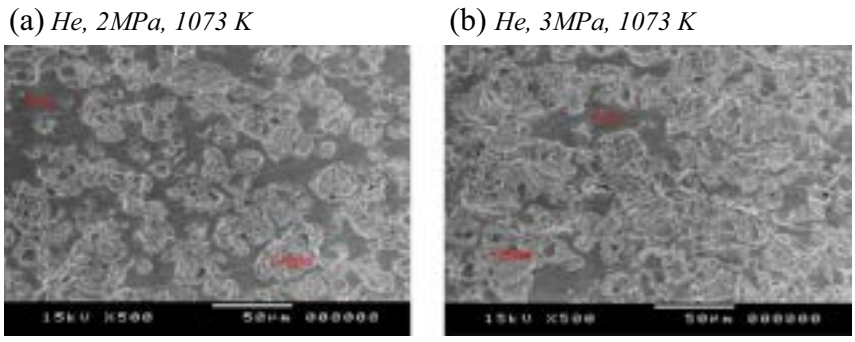

Fig. 16. Surface of SS 316 L substrates after fracture.

5. Conclusions

In this study, Cu coatings were prepared with cold spray process under different spray conditions onto three different substrates. Then, adhesive strength on three substrates was tested. Splat was also observed in order to understand the bonding mechanism. An ultra-strong adhesive strength (more than 200 MPa) of Cu coatings on Al5052, Al6063 and stainless steel 316 L substrates was obtained with cold spray processing by improving the particle impact velocity.

Plastic energy from the initial impact kinetic energy is primarily dissipated in the soft counterpart of substrate and particle. Therefore, for Al alloy substrates, the deformation mainly occurred in the substrate, in which resulted in the formation of a deeply embedded splat. Jetting was formed by the substrate deformation with the increase of embedded depth due to the high particle velocity. Higher particle velocity generated stronger bonding strength between the coatings and Al alloy substrates mainly owing to the improvement of mechanical interlock effect. In contrast, the deformation mainly generates in the Cu particle instead of the substrate on stainless steel 316 L substrate. Effective bonding can be formed based on the diffusion between Cu coating and stainless steel substrate to generate a metallurgical bonding. The ultra-strong adhesive strength between Cu coating and stainless steel can be possible if high particle velocity is achieved.

References

[1] A. Papyrin, V. Kosarev, K.V. Klinkov, A. Alkhimov, V.M. Fomin, Cold Spray Technology, Elsevier, Oxford, 2006.
[2] C.-J. Li, H.-T. Wang, Q. Zhang, G.-J. Yang, W.-Y. Li, H.L. Liao, J. Therm. Spray Technol. 19 (1–2) (2010) 95–101.
[3] C.-J. Li, W.-Y. Li, Y.-Y. Wang, in: B.R. Marple, C. Moreau (Eds.), Thermal Spray 2003: Advancing the Science and Applying the Technology, ASM International, Materials Park, OH, 2003, pp. 91–95.
[4] F. Raletz, M. Vardelle, G. Ezo'o, Surf. Coat. Technol. 201 (5) (2006) 1942–1947.
[5] J. Voyer, T. Stoltenhoff, H. Kreye, in: B.R. Marple, C. Moreau (Eds.), Thermal Spray 2003: Advancing the Science and Applying the Technology, ASM International, Materials Park, OH, 2003, pp. 71–78.
[6] H. Mäkinen, J. Lagerbom, P. Vuoristo, in: B.R. Marple, M.M. Hyland, Y.-C. Lau, C.-J. Li, R.S. Lima, G. Montavon (Eds.), Thermal Spray 2007: Global Coating Solutions, May 14–16, 2007, ASM International, 2007, pp. 31–36.
[7] K.-R. Donner, R. Roedel, F. Gärtner, T. Klassen, Thermal Spray 2011: Proceedings of the International Thermal Spray Conference, DVS-ASM, September 2011, pp. 72–77.
[8] M. Grujicica, J.R. Saylor, D.E. Beasley, W.S. DeRosset, D. Helfritch, Appl. Surf. Sci. 219 (3–4) (2003) 211–227.
[9] S. Kumar, G. Bae, C. Lee, Appl. Surf. Sci. 255 (6) (2009) 3472–3479.
[10] M. Grujicic, C.L. Zhao, W.S. Derosset, D. Helfritch, Mater. Des. 25 (2004) 681–688.
[11] S. Guetta, M.H. Berger, F. Borit, V. Guipont, M. Jeandin, M. Boustie, Y. Ichikawa, K. Sakaguchi, K. Ogawa, J. Therm. Spray Technol. 18 (3) (2009) 331–342.
[12] W. Li, H. Liao, C. Li, H. Bang, C. Coddet, Appl. Surf. Sci. 253 (11) (2007) 5084–5091.
[13] S. Yin, X. Wang, X. Suo, H. Liao, Z. Guo, W. Li, C. Coddet, Acta Mater. 61 (14) (2013) 5105–5118.
[14] R.C. Dykhuizen, M.F. Smith, D.L. Gilmore, R.A. Neiser, X. Jiang, S. Sampath, J. Therm. Spray Technol. 8 (4) (1999) 559–564.
[15] T. Schmidt, F. Gärtner, T. Stoltenhoff, H. Kreye, H. Assadi, Thermal Spray 2005: Thermal Spray connects: explore its surfacing potential, DVS-ASM, 2005, pp. 232–238.
[16] T. Hussain, D.G. McCartney, P.H. Shipway, D. Zhang, J. Therm. Spray Technol. 18 (3) (2009) 364–379.
[17] W.-Y. Li, C.-J. Li, G.-J. Yang, Appl. Surf. Sci. 257 (5) (2010) 1516–1523.
[18] X.-J. Ning, J.-H. Kim, H.-J. Kim, C. Lee, Appl. Surf. Sci. 255 (2009) 3933–3939.
[19] T. Schmidt, H. Assadi, F. Gartner, H. Richter, T. Stoltenhoff, H. Kreye, T. Klassen, J. Therm. Spray Technol. 18 (5–6) (2009) 794–808.
[20] T.W. Clyne, S.C. Gill, J. Therm. Spray Technol. 5 (4) (1996) 401–418.
[21] A.M. Kamara, K. Davey, Int. J. Solids Struct. 44 (25–26) (Dec. 2007) 8532–8555.
[22] H. Fukanuma, N. Ohno, A study of adhesive strength of cold spray coatings, Thermal Spray 2004: Advances in Technology and Applications (ASM International), Osaka, Japan, May 10–12, 2004, pp. 329–334.
[23] V.K. Champagne, The Cold Spray Materials Deposition Process: Fundamentals and Applications, Woodhead Publishing, Sep. 2007. 2.
[24] I. Smurov, D. Pervushin, V. Ulianitsky, S. Zlobin, A. Sova, Comparison of Cold Spray and Detonation Coatings Properties, International Thermal Spray Conference & Exposition, Thermal Spray: Global Solutions for Future Application (DVS-ASM), Singapore, May 03–05, 2010, pp. 487–490.
[25] R. Huang, H. Fukanuma, Japan Society of Mechanical Engineers (JSME) annual meeting, 6, 2010, pp. 425–426, (In Japanese).
[26] R. Huang, H. Fukanuma, J. Therm. Spray Technol. 21 (3–4) (2012) 541–549.
[27] T. Marrocco, D.G. McCartney, P.H. Shipway, A.J. Sturgeon, J. Therm. Spray Technol. 15 (2) (2006) 263–272.
[28] A. Shapiro, The Dynamics and Thermodynamics of Compressible Fluid Flow, Roland Press, New York, 1953.
[29] D. Helfritch, V. Champagne, Proceedings of the Army Science Conference (26th), Orlando, Florida, December 2008.
[30] R.C. Dykhuizen, M.F. Smith, J. Therm. Spray Technol. 7 (2) (1998) 205–212.
[31] K. Nakamura, H. Amita, S. Takahashi, S. Matsumoto, J. Surf. Anal. 15 (1) (2008) 50–58.
[32] G. Bae, Y. Xiong, S. Kumar, K. Kang, C. Lee, Acta Mater. 56 (17) (2008) 4858–4868.
[33] C. Chen, H. Chen, W. Hwang, Mater. Trans. 47 (4) (2006) 1232–1239.
[34] H. Fukanuma, N. Ohno, in: C. Moreau, B. Marple (Eds.), Thermal Spray 2003: Advancing the Science & Applying the Technology, ASM International, Materials Park, Ohio, USA, 2003, pp. 1361–1368.
[35] O.R. Bagnato, D.V. Freitas, F.R. Francisco, F.E. Manoel, T. Alonso, Proceedings of IPAC'10, Kyoto, Japan, 2010, pp. 3975–3977.
[36] S.-X. Lia, F.-Z. Xuan, S.-T. Tung, S.-R. Yu, Mater. Sci. Eng. A 491 (2008) 488–491.
[37] Y. Kaya, N. Kahraman, A. Durgutlu, B. Gülenç, Proc. IME B J. Eng. Manufact. 226 (3) (March 2012) p478–p484.